

Comparison Between the Variational and Implicit Differentiation Approaches to Shape Design Sensitivities

R. J. Yang* and M. E. Botkin†

General Motors Research Laboratories, Warren, Michigan

The most commonly used approach to the shape design sensitivity problem results from the implicit differentiation of the discretized equilibrium equations. The most general implementation of this technique requires that finite differences be used to differentiate the element stiffness matrices. Proper choice of the step size is necessary to obtain high levels of accuracy and to avoid round-off errors. Furthermore, since it is necessary to operate on the element matrices, this method is difficult to implement into a general-purpose finite element program. A more recent shape design sensitivity formulation, based upon variational calculus, avoids having to differentiate the discretized equations and results in an analytical expression for the derivative. The approach is based upon the total derivative of the variational state equation and uses an adjoint variable technique for design sensitivity analysis. Only structural response data on the boundary of the structure is necessary, thereby making implementation into a general-purpose program less difficult. This paper attempts to compare the two different techniques and point out the similarities. Two test problems are shown to demonstrate the accuracy of the variational approach.

Introduction

SHAPE optimal design is an important class of structural design problems in which the shape of a two- or three-dimensional structural component is to be determined, subject to constraints involving natural frequencies, displacements, and stresses in the structure. One difficulty in shape optimization is due to the inaccurate performance derivative calculation. Also, in general, the performance derivative that is essential in the use of any direct optimization technique, cannot be obtained analytically. A finite difference scheme, using the implicit differentiation method, is widely used in the structural optimization world.¹⁻⁴ In this scheme, the discretized equilibrium equation of the structure is first differentiated. The performance change is then obtained by varying each design variable by a specific amount. The advantages of this approach are its generality and simplicity. A disadvantage is that one has to choose a proper step size change for the design parameters. The choice of step size is artistic; a poor choice may cause numerical difficulty due to round-off error and nonlinearity of structural performances. An additional drawback with the implicit differentiation approach for shape variables is the difficulty in its implementation into a general-purpose finite element program.

Haug et al.⁵⁻⁸ developed a unified theory of structural design sensitivity analysis for linear elastic structures, using a variational formulation of the structural equations. This theory allows one to take the total derivative, or material derivative, of the variational state equation and to use an adjoint variable technique for design sensitivity analysis. The main attraction of this approach is that it allows one to compute the derivatives of structural performances analytically. No discretization approximations are involved during the derivation and the step size need not be specified in the calculation. However, the formulation requires evaluating accurate stress quantities on the boundaries which are often difficult to obtain.

In this paper, the variational design sensitivity formulation is interpreted and the formulation is related to the implicit differentiation approach. Two examples are given to illustrate the use of the variational approach and to compare the results of the two different approaches.

Implicit Differentiation Approach (IDA)

A structural system can be discretized to obtain the equilibrium equation as

$$Kz = F \quad (1)$$

where K is the reduced global stiffness matrix and z and F the displacement and force vectors, respectively. If one implicitly differentiates the equilibrium equation with respect to a shape design variable vector b and assumes that force vector F is independent of b , the following result is obtained:

$$\frac{\partial z}{\partial b_i} = -K^{-1} \frac{\partial K}{\partial b_i} z$$

or

$$\Delta z = -K^{-1} \Delta K z \quad (2)$$

Traditionally, the calculation of $\partial(K)/\partial b_i$ is done by either analytically carrying out the differentiation⁹ or performing a numerical finite difference calculation. When the finite difference calculation is performed for the shape design sensitivity, one is actually comparing two separate finite element meshes and effectively evaluating changes in the finite element mesh discretization as well as the boundary change. In general, the stiffness matrix K or strain recovery matrix B is sufficiently complex to preclude analytical evaluation of the derivative for shape optimization. Also, the analytical derivative tends to be element dependent, whereas the finite difference approach is not. For conventional or nonshape structural optimization, i.e., area, thickness, or material properties as design variables, analytical derivatives may be obtained in some cases.

Variational Design Sensitivity Analysis (VDSA)

Variational Formulation

Since the shape of domain Ω of a structural component is treated as the design variable, it is convenient to think of Ω

Received May 13, 1985; revision received Sept. 9, 1985. Copyright © American Institute of Aeronautics and Astronautics, Inc., 1986. All rights reserved.

*Senior Research Engineer, Engineering Mechanics Department.

†Senior Staff Research Engineer, Engineering Mechanics Department.

as a continuous medium and to utilize the material derivative idea from continuum mechanics. The pointwise material derivative (if it exists) at $x \in \Omega$ is defined as⁷

$$\begin{aligned}\dot{z}(x) &\equiv \frac{d}{d\tau} z_\tau(x, \tau V(x))|_{\tau=0} \\ &= \lim_{\tau \rightarrow 0} \frac{z_\tau(x + \tau V(x)) - z(x)}{\tau}\end{aligned}\quad (3)$$

where τ is the parameter defining the transformation between initial and current shapes, which can be thought of as time, and $V(x)$ the design perturbation and may be thought of as a design deformation velocity.

If z_τ has a regular extension in a neighborhood of $\bar{\Omega}$, then one has

$$\dot{z}(x) = z'(x) + \nabla z^T V(x) \quad (4)$$

where

$$z'(x) \equiv \lim_{\tau \rightarrow 0} \frac{z_\tau(x) - z(x)}{\tau} \quad (5)$$

is the partial derivative of z and ∇ is a gradient symbol.

The material derivatives of a functional ψ , which is usually also taken as a structural performance measure, can be defined as

$$\dot{\psi} \equiv \frac{d}{d\tau} \psi(\tau)|_{\tau=0} = \lim_{\tau \rightarrow 0} \frac{\psi(\tau) - \psi(0)}{\tau} \quad (6)$$

Specifically, one defines ψ as

$$\psi = \int_{\Omega_\tau} f_\tau(x_\tau) d\Omega_\tau \quad (7)$$

where f_τ is a regular function defined in Ω_τ and subscript τ denotes the deformed configuration. Using Eq. (6), the material derivative of ψ is^{6,7}

$$\dot{\psi} = \int_{\Omega} f'(x) d\Omega + \int_{\Gamma} f(x) V^T n d\Gamma \quad (8)$$

where n is a outward unit normal vector of boundary Γ .

In Eq. (6), one sees that the term material derivative is a misnomer and is actually a differential. This is not obvious from the definition of the material derivative. To better understand this, one may first consider the derivative of a real valued function of a real variable and then extend it to the derivative of a functional of a function.

Let u map a real set \mathcal{R} to another set \mathcal{R} , i.e., $\mathcal{R} \rightarrow \mathcal{R}$, and the definition of the derivative is

$$u'(x_0) = \lim_{\alpha \rightarrow 0} \frac{u(x_0 + \alpha) - u(x_0)}{\alpha}$$

or

$$u'(x_0)(x - x_0) = \lim_{\alpha \rightarrow 0} \left\{ \frac{u(x_0 + \alpha) - u(x_0)}{\alpha} (x - x_0) \right\} \quad (9)$$

Writing $x - x_0 = \eta$, and replacing α by $\alpha\eta$, one then has

$$u'(x_0)\eta = \lim_{\alpha \rightarrow 0} \frac{u(x_0 + \alpha\eta) - u(x_0)}{\alpha} \quad (10)$$

One then clearly sees that the right-hand side of Eq. (10) is a differential, not a derivative, since $u'(x_0)$ is the derivative at point x_0 and η is a difference of $x - x_0$. This interpretation can be expanded to function space and to the so-called

Gateaux derivative.^{10,11} The material derivative is, in fact, a kind of Gateaux derivative; thus, it is a differential quantity and not an ordinary derivative.

Another way to see this fact is to simply define the volume of a solid as a functional

$$\psi = \int_{\Omega} d\Omega \quad (11)$$

When taking the material derivative of Eq. 11, one has

$$\dot{\psi} = \int_{\Gamma} V^T n d\Gamma \quad (12)$$

Then, one clearly observes that the right side of Eq. (12) represents the change of volume, instead of rate of volume change.

Consider a displacement functional at an isolated fixed point \bar{x} , i.e.,

$$\psi = \int_{\Omega} \delta(x - \bar{x}) z d\Omega \quad (13)$$

where δ is the Dirac measure at zero and the state variable or displacement z is governed by the variational equation,

$$a(z, \bar{z}) \equiv \int_{\Omega} \sigma^{ij}(z) \epsilon^{ij}(\bar{z}) d\Omega = \int_{\Gamma^2} T_i \bar{z}_i d\Gamma \quad (14)$$

where $a(z, \bar{z})$ is the energy bilinear form, σ^{ij} and ϵ^{ij} the stress and strain tensors, respectively, Γ^2 the loaded boundary, T_i the traction vector, and \bar{z} a kinematically admissible virtual displacement. Note that the summation convention for a repeated index is used throughout this paper.

The differentiability results for the energy bilinear forms, static response, and constraint functional were used to develop the shape design sensitivity formulas. Since the proofs, found in Ref. 7, are tedious and do not contribute insight into the adjoint variable technique, the derivations are not repeated here.

One can take material derivatives of both Eqs. (13) and (14) by assuming that the actual load and the corresponding boundary are unchanged during the deformation and applying the adjoint variable method to obtain

$$\begin{aligned}\dot{\psi} &= \int_{\Gamma^0} \{ \sigma^{ij}(\lambda) \nabla z_i^T V + \sigma^{ij}(z) \nabla \lambda_j^T V \} n_j d\Gamma \\ &\quad - \int_{\Gamma} \sigma^{ij}(z) \epsilon^{ij}(\lambda) V^T n d\Gamma\end{aligned} \quad (15)$$

where Γ^0 and Γ denote kinematically constrained and moving boundaries, respectively, and the adjoint variable λ is governed by

$$a(\lambda, \bar{\lambda}) = \int_{\Omega} \delta(x - \bar{x}) \bar{\lambda} d\Omega \quad (16)$$

where $\bar{\lambda}$ is a kinematically admissible virtual displacement. One may notice that the discretized stiffness matrices for the equilibrium equation (14) and the adjoint equation (16) are identical, since the energy bilinear forms are the same and both \bar{z} and $\bar{\lambda}$ are in the same space of kinematically admissible displacements. Physically, the adjoint equation (16) is interpreted by simply applying a unit load at the point where the displacement is of interest. The detailed derivation can be found in Refs. 5-7.

Numerical Interpretation

For simplicity, one can assume that the kinematically constrained boundary is fixed, Eq. (15) then becomes

$$\dot{\psi} = - \int_{\Gamma} \sigma^{ij}(z) \epsilon^{ij}(\lambda) V^T n d\Gamma \quad (17)$$

One may notice that in Eq. (17), only the boundary integral appears and that it is computable once the boundary stresses, strains, and velocity are available.

When the shape design parameter vector b is defined, it can be linearized in terms of δb by

$$b = b^0 + \tau \delta b \quad (18)$$

where b^0 is the nominal design at the given iteration. Presume that points on the boundary Γ are specified by a position vector $r(b)$, then the velocity field at the boundary is defined by using Eq. (18), as⁵

$$V \equiv \frac{d}{d\tau} [r(b)] = \frac{\partial r}{\partial b} \delta b \quad (19)$$

Substituting V into Eq. (17) and rewriting the lefthand side, one obtains

$$\begin{aligned} \frac{\partial \psi}{\partial b} \delta b &= - \int_{\Gamma} \sigma^{ij}(z) \epsilon^{ij}(\lambda) n^T \frac{\partial r}{\partial b} \delta b d\Gamma \\ &= - \left(\int_{\Gamma} \sigma^{ij}(z) \epsilon^{ij}(\lambda) n^T \frac{\partial r}{\partial b} d\Gamma \right) \delta b \end{aligned} \quad (20)$$

Finally, the gradient of a displacement can be rewritten as

$$\frac{\partial \psi}{\partial b} = - \int_{\Gamma} \sigma^{ij}(z) \epsilon^{ij}(\lambda) n^T \frac{\partial r}{\partial b} d\Gamma \quad (21)$$

Note that in Eq. (21), once the physical boundary is parameterized, i.e., $\partial r / \partial b$ is known, the derivative of a displacement can be computed, using boundary information only. The design variable step size δb disappears in Eq. (21), while it is needed and crucial in the finite difference approach for the implicit differential method.

Relationship Between IDA and VDSA

In order to obtain the design sensitivity of Eq. (17), one has to solve Eq. (14) for the state variable z and Eq. (16) for the adjoint variable λ . As mentioned before, physically, λ is obtained by applying a unit load at the nodal point where the displacement is of interest. If all the displacement derivatives are desired, then λ is an $N \times N$ matrix, instead of an $N \times 1$ vector, where N is the total number of degrees of freedom of the system. The discretized adjoint equation for variable λ is then written as

$$K\lambda = I \quad (22)$$

where I is the identity matrix. One may notice that the λ is simply the flexibility matrix or inverse of the stiffness matrix K^{-1} from finite element analysis. A similar interpretation also can be found in Ref. 12. However, the definition for the adjoint variable is different by a minus sign. Applying this observation to Eq. (17), a formula similar to Eq. (2) can be obtained.

First, the actual stresses and adjoint strains in Eq. (17) can be expressed as

$$\sigma(z) = DBz_e \quad \epsilon(\lambda) = B\lambda_e \quad (23)$$

where D is the elasticity matrix, B the strain recovery matrix, and subscript e the elemental displacement, which is related to the global displacement vector by a transformation matrix β , as

$$z_e = \beta z \quad (24)$$

Equation (17) then is discretized to a computable finite element form as

$$\delta \psi = - \sum_{N_b} \int_{\Gamma} z^T C \lambda V^T n d\Gamma \quad (25)$$

where $C = \beta^T B^T D B \beta$ and N_b is the boundary element number. In Eq. (25), C is a $N \times N$ symmetric matrix; thus, λ and z are interchangeable. Replacing λ by K^{-1} , one obtains

$$\delta \psi = -K^{-1} \left(\sum_{N_b} \int_{\Gamma} C V^T n d\Gamma \right) z \quad (26)$$

Note that in Eq. (26), $V^T n$ is the normal movement of the solid boundary, and thus it can be interpreted as a domain change $d\Omega_+$, in an infinitesimal sense. Equation (26), then, can be rewritten as

$$\delta \psi \approx -K^{-1} \left(\sum_{N_b} \int_{\Omega} C d\Omega_+ \right) z \quad (27)$$

Comparing Eqs. (27) and (2), one obtains

$$\left(\Delta K - \sum_{N_b} \int_{\Omega} C d\Omega_+ \right) z = 0 \quad (28)$$

Note that from Eq. (1),

$$z = K^{-1} F \quad (29)$$

Since K is a nonsingular matrix, one can make z arbitrary in the space R^n by arbitrarily varying F . This result implies that

$$\Delta K \approx \sum_{N_b} \int_{\Omega} C d\Omega_+ \quad (30)$$

One should notice that Eq. (30) is valid only when the finite element mesh remains unperturbed, i.e., only the boundary nodes are allowed to move, since in Eq. (27) all information is transformed to the boundary and as a result the internal node effects are excluded automatically.

This approximation to ΔK has been proposed by Zienkiewicz and Campbell,¹³ who pointed out that the major effect on stiffness change is due to the change of area of integration rather than the change of $\beta^T B^T D B \beta$, or the C matrix, in Eq. (25). Thus, the variational formulation can be related to the implicit differentiation approach for a change of the traction-free boundary. As for kinematically constrained boundaries, Eq. (17) is no longer valid. Instead, Eq. (15), which includes an additional term on Γ^0 , should be employed. However, it has not been proved here that both approaches are equivalent in this case.

It is worthwhile to notice that the derivatives computed by the variational approach, namely Eqs. (15) and (17), are based on boundary information only. This implies that the accuracy of design sensitivity depends on accurate boundary information. A better estimation of the boundary stresses leads to a more accurate design sensitivity estimate. Conversely, if the stiffness matrix is to be differentiated as in the IDA method, accurate calculation of the stiffness matrix is required. Numerical results are shown in the next section to demonstrate this fact.

Another way to relate the two approaches is to directly take the material derivative of the discretized equilibrium equation of Eq. (1) to obtain

$$\frac{Dz}{D\tau} = -K^{-1} \frac{DK}{D\tau} z \quad (31)$$

and

$$\frac{DK}{D\tau} = \sum_{N_e} \left\{ \int_{\Omega} \frac{\partial C}{\partial \tau} d\Omega + \int_{\Gamma} CV^T n d\Gamma \right\} \quad (32)$$

where N_e is the number of finite elements. Using the fact that $\partial C/\partial \tau = 0$ and assuming the interelemental boundary is fixed, Eq. (29) becomes

$$\Delta z = -K^{-1} \left(\sum_{N_b} \int_{\Gamma} CV^T n d\Gamma \right) z \quad (33)$$

Note that Eq. (33) is identical to Eq. (26), which is obtained from variational design sensitivity theory. Recall that Eq. (26) is valid only for the traction-free boundary, while Eq. (32) does not imply this condition. However, Eq. (33) is derived from the discretized equilibrium equation, in which the kinematical boundary conditions are already imposed to obtain the reduced stiffness matrix K . This may automatically exclude the possibility of moving a kinematically constrained boundary.

The relationship between IDA and VDSA shown in this section was valid only for problems with homogeneous kinematical boundary conditions.

Numerical Examples

Two examples are discussed in this section. The results are obtained based on the assumption that the interelement boundary is fixed.

A Two-Dimensional Thin Plate¹⁴

A simple two-dimensional thin plate is considered as an example to demonstrate the use of the variational design sensitivity theory and the boundary parameterization and to compare the two approaches discussed in the previous sections. The finite element configuration, dimensions, material properties, loading condition, and design variable are shown in Fig. 1. Design variable b is chosen to move the upper boundary, i.e., the traction-free boundary. Thus, $n^T \partial r / \partial b$ of Eq. (21) is equal to 1, and Eq. (21) is reduced to

$$\frac{\partial \psi}{\partial b} = - \int_{\Gamma} \sigma^{ij}(z) \epsilon^{ij}(\lambda) d\Gamma \quad (34)$$

An eight-noded isoparametric plane stress element is employed for analysis. The boundary stresses and strains that appear in Eq. (34) are computed by extrapolating linearly from the stresses at the Gaussian points, where the optimal or the best approximate stresses are located.¹⁵ An external load of 100 lb is parabolically applied at the right end of the solid.

Numerical results for design sensitivity of point A in the Y direction for 1×1 , 2×2 , 3×3 , 4×4 , 5×5 , and 6×6 meshes are shown in Table 1.

In Table 1, column 2 represents the displacement in Y direction for the initial design b . Column 3 shows the value of the displacement derivative at point A for the implicit approach (IDA) that evaluates the stiffness derivative analytically, column 4 is the IDA result by finite difference method that uses $0.001b$ as the step size, and column 5 is the result for the variational approach (VDSA).

Figure 2 shows the same results as in Table 1. From Fig. 2 and Table 1, one observes that the displacements and the sensitivities for the implicit approach, either analytical or finite difference methods, do not change much after 3×3 finite element mesh. However, the design sensitivity for the VDSA is still increasing as the finite element mesh increases. This implies that the variational approach is more sensitive to the finite element results, although it provides the analytical formulation for sensitivities.

From this simple example, one concludes that the variational approach tends to yield better gradient estimates, once a more accurate analysis is used and better boundary stresses are obtained. The same conclusion is also found in Ref. 16.

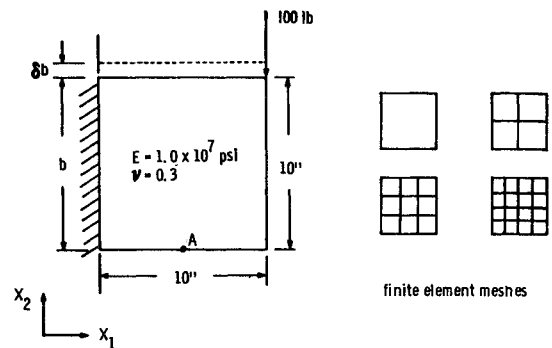


Fig. 1 Square thin plate.

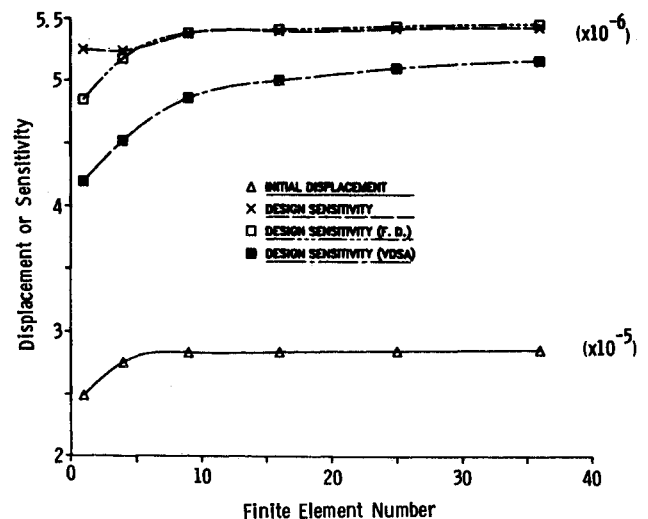


Fig. 2 Accuracy of design sensitivity.

Table 1 Accuracy of design sensitivity

Element	ν	IDA dv/db	IDA (finite difference) dv/db	VDSA dv/db
1×1	2.495E-5	-5.248E-6	-4.845E-6	-4.196E-6
2×2	2.760E-5	-5.235E-6	-5.173E-6	-4.518E-6
3×3	2.841E-5	-5.375E-6	-5.381E-6	-4.856E-6
4×4	2.845E-5	-5.394E-6	-5.409E-6	-4.995E-6
5×5	2.854E-5	-5.413E-6	-5.436E-6	-5.093E-6
6×6	2.856E-5	-5.426E-6	-5.456E-6	-5.158E-6

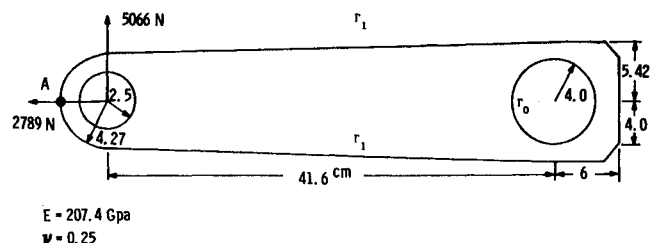
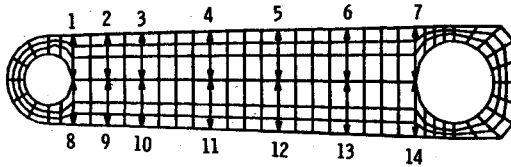


Fig. 3 Automotive torque arm.

Table 2 Design sensitivity of torque arm

Variable	z_1	z_2	Δz	VDSA		IDA (finite difference)	
				Δz_v	Error, %	Δz_i	Error, %
1	0.2429	0.2429	-7.527E-6	-7.432E-6	-1.3	-1.076E-4	43.0
2	0.2429	0.2429	-2.524E-6	-2.605E-6	3.2	-5.180E-5	105.2
3	0.2429	0.2429	-1.583E-5	-1.587E-5	0.2	-1.921E-4	21.3
4	0.2429	0.2429	-4.061E-5	-4.063E-5	0.1	-4.323E-4	6.5
5	0.2429	0.2428	-6.719E-5	-6.730E-5	0.2	-6.887E-4	2.5
6	0.2429	0.2428	-1.040E-4	-1.039E-4	-0.1	-1.048E-3	0.8
7	0.2429	0.2428	-8.319E-5	-8.215E-5	-1.2	-8.356E-4	0.5



Note: numbers denote shape design parameters

Fig. 4 Design variables and finite element of torque arm.

An Automotive Torque Arm

An automotive rear suspension torque arm studied in Ref. 4 is analyzed in this section, with the geometry, loading conditions, and material properties shown in Fig. 3. For simplicity, a single, nonsymmetric, in-plane static load and plane stress are considered. Zero displacement constraints are applied around the larger hole on the right, in order to simulate attachment to a solid rear axle. Thickness is kept constant at 0.3 cm. The shapes of Γ_1 , both the upper and lower portions, are to be determined through the optimization process. The other boundary segments are kept fixed.

Consider the variable boundary Γ_1 of the torque arm shown in Fig. 3, which can be characterized as a curve $x_2 = f(x_1)$ in which a small vertical variation $\delta f(x_1)$ is allowed. The normal movement of the boundary can be written as

$$V^T n = \delta f n_2 = \delta \left(-\frac{dx_1}{ds} \right) \quad (35)$$

where s is arc length on Γ_1 , which is measured counterclockwise. Thus, the sensitivity formula of Eq. (17) can be rewritten as

$$\delta \psi = \int_{\Gamma_1} \sigma_{ij}^u(z) \epsilon_{ij}^u(\lambda) \delta f dx_1 \quad (36)$$

In Eq. (36), δf can be easily related to δb , once the curve Γ_1 defined by $x_2 = f(x_1)$ is parameterized by a design variable vector b .

A spline function having two continuous derivatives everywhere and characteristics of global smoothness is employed. Design variables are the distances between the central line and boundary points, shown in Fig. 4. The upper and lower portions of the boundary each have seven design variables. Detailed spline represented boundary parameterization can be found in Ref. 16.

The finite element model shown in Fig. 4 includes 204 elements, 707 nodal points, and 1342 degrees of freedom. The design sensitivity for vertical displacement of the left end (point A) is computed using both variational and implicit differentiation methods. The extrapolation strategy for boundary stresses is employed in this case. Results by varying each design variable of the upper boundary by 0.1%, i.e., from 1 to 7, are shown in Table 2.

One observes that in Table 2, the variational approach, in general, yields a better estimate (column 6) than the implicit differentiation approach (column 8). The inaccurate estimate for the implicit method, using finite differences, is due to the difference error for ΔK , since some design variable changes result in only small changes of K . The fact is shown in Table 2, where one observes that a smaller Δz leads to a less accurate estimate (column 8). On the other hand, the good estimate for the variational approach results from the accuracy of the finite element model and the linearity of the system with respect to the design variables. Since this model includes 204 eight-noded isoparametric elements and 1342 degrees of freedom, a reasonably accurate solution is ensured. This confirms that accurate analysis is needed in order to obtain good design sensitivities using the variational approach. This also indicates that quality control of the finite element solution is needed in shape optimal design.

Two procedures can be employed for calculation of the performance derivatives, using the implicit differentiation method. The analytical procedure (example 1) evaluates the true derivative from the derivatives of the nodal coordinates with respect to the shape design variables. Since it requires the relationship between nodal points and shape design parameters and tends to be element dependent, this approach may not be practical for a wide range of problems. The finite difference procedure has the advantage of generality and has been widely used. However, there are two drawbacks: 1) the approximate derivatives may be inapplicable for optimization, when the system is highly nonlinear or large design changes are used; and 2) the round-off error in calculating the difference may become significant, when a small design change is used (example 2) or an improper shape design variable is chosen. This may result in undesirable derivatives and a slow rate of convergence, if the problem converges at all.

Summary

Two approaches for obtaining sensitivities of structural response with respect to shape variation have been reviewed and compared. The most well-known method is obtained from implicit differentiation of the finite element equations of equilibrium. This formulation requires either the analytical derivative of an element stiffness matrix with respect to shape variation or a finite difference approximation of the derivative. Either of these quantities is difficult to obtain from a general-purpose finite element program for which the source is not available. More recently, a new theory has been developed in which one takes the material derivative of the variational state equation and uses an adjoint variable technique for design sensitivity analysis. The advantage of this approach is that an analytical expression for the sensitivities is obtained which is dependent upon only the boundary solution quantities generally available from general-purpose programs. The primary disadvantage is that these quantities are difficult to obtain accurately. It was shown in this paper that, by introducing the discrete finite element expressions for stresses and strains into the varia-

tional formulation for sensitivities, the two approaches result in the same matrix equation. Certain assumptions were made limiting this relationship to unconstrained and unloaded boundaries. In this matrix equation, the term in the variational approach, which represents the stiffness change in the area of integration and does not include the change in the terms of the strain recovery matrix.

Two demonstration problems were presented in which comparisons were made between the accuracy of the two approaches. In general, it was observed that, although the variational formulation does not directly depend upon the finite element method and is considered to be the more accurate of the two approaches, it does depend on the finite element results for the needed boundary solution information. As a result, the accuracy tends to be indirectly affected by the finite element solution. The primary deficiency in the implicit differentiation approach comes when finite differences are employed in the computation of the stiffness matrix derivatives, in that it is difficult to select the correct step size to avoid inaccuracies.

References

- ¹Bennett, J. A. and Botkin, M. E., "Structural Shape Optimization with Geometric Description and Adaptive Mesh Refinement," *AIAA Journal*, Vol. 23, March 1985, pp. 458-464.
- ²Botkin, M. E., "Adaptive Finite Element Mesh Technique for Plate Structures," *AIAA Journal*, Vol. 23, May 1985, pp. 812-814.
- ³Botkin, M. E. and Bennett, J. A., "Shape Optimization of Three-Dimensional Folded Plate Structures," *AIAA Journal*, Vol. 23, Nov. 1985, pp. 1804-1810.
- ⁴Botkin, M. E., "Shape Optimization of Plate and Shell Structures," *AIAA Journal*, Vol. 20, Feb. 1982, pp. 268-273.
- ⁵Haug, E. J., Choi, K. K., Hou, J. W., and Yoo, Y. M., "A Variational Method for Shape Optimal Design of Elastic Structures," *New Directions in Optimum Structural Design*, edited by E. Atrek et al., John Wiley & Sons, New York, 1984, pp. 105-137.
- ⁶Choi, K. K. and Haug, E. J., "Shape Design Sensitivity Analysis of Elastic Structures," *Journal of Structural Mechanics*, Vol. 11, No. 2, 1983, pp. 231-269.
- ⁷Haug, E. J., Choi, K. K., and Komkov, V., *Design Sensitivity Analysis of Structural Systems*, Academic Press, New York, 1986.
- ⁸Choi, K. K., "Shape Design Sensitivity Analysis of Displacement and Stress Constraints," *Journal of Structural Mechanics*, Vol. 13, No. 1, 1985, pp. 27-41.
- ⁹Ramakrishnan, C. V. and Francavilla, A., "Structural Shape Optimization Using Penalty Functions," *Journal of Structural Mechanics*, Vol. 3, No. 4, 1974-1975, pp. 403-422.
- ¹⁰Choi, K. K., Personal communication, 1984.
- ¹¹Curtain, R. F. and Pritchard, A. J., *Functional Analysis in Modern Applied Mathematics*, Academic Press, New York, 1977.
- ¹²Belegundu, A. D. and Arora, J. S., "A Sensitivity Interpretation of Adjoint Variables in Optimal Design," *Computer Methods in Applied Mechanics and Engineering*, Vol. 48, 1985, pp. 81-89.
- ¹³Zienkiewicz, O. C. and Campbell, J. C., "Shape Optimization and Sequential Linear Programming," *Optimum Structural Design*, edited by R. H. Gallagher and O. C. Zienkiewicz, John Wiley & Sons, New York, 1973.
- ¹⁴Schmit, L. A., Personal communication, 1984.
- ¹⁵Barlow, J., "Optimal Stress Locations in Finite Element Models," *International Journal for Numerical Methods in Engineering*, Vol. 10, 1976, pp. 243-251.
- ¹⁶Yang, R. J. and Choi, K. K., "Accuracy of Finite Element Based Shape Design Sensitivity Analysis," *Journal of Structural Mechanics*, Vol. 13, No. 2, 1985.

From the AIAA Progress in Astronautics and Aeronautics Series . . .

COMBUSTION EXPERIMENTS IN A ZERO-GRAVITY LABORATORY—v. 73

Edited by Thomas H. Cochran, NASA Lewis Research Center

Scientists throughout the world are eagerly awaiting the new opportunities for scientific research that will be available with the advent of the U.S. Space Shuttle. One of the many types of payloads envisioned for placement in earth orbit is a space laboratory which would be carried into space by the Orbiter and equipped for carrying out selected scientific experiments. Testing would be conducted by trained scientist-astronauts on board in cooperation with research scientists on the ground who would have conceived and planned the experiments. The U.S. National Aeronautics and Space Administration (NASA) plans to invite the scientific community on a broad national and international scale to participate in utilizing Spacelab for scientific research. Described in this volume are some of the basic experiments in combustion which are being considered for eventual study in Spacelab. Similar initial planning is underway under NASA sponsorship in other fields—fluid mechanics, materials science, large structures, etc. It is the intention of AIAA, in publishing this volume on combustion-in-zero-gravity, to stimulate, by illustrative example, new thought on kinds of basic experiments which might be usefully performed in the unique environment to be provided by Spacelab, i.e., long-term zero gravity, unimpeded solar radiation, ultra-high vacuum, fast pump-out rates, intense far-ultraviolet radiation, very clear optical conditions, unlimited outside dimensions, etc. It is our hope that the volume will be studied by potential investigators in many fields, not only combustion science, to see what new ideas may emerge in both fundamental and applied science, and to take advantage of the new laboratory possibilities.

Published in 1981, 280 pp., 6×9, illus., \$25.00 Mem., \$39.00 List

TO ORDER WRITE: Publications Order Dept., AIAA, 1633 Broadway, New York, N.Y. 10019